American Journal of Applied Mathematics
2026, Vol. 14, No. 4, pp. 174–185
https://doi.org/10.11648/j.ajam.20261404.11

Research Article

A Caputo Fractional-Order Model for Breast Cancer Tumor–Immune Dynamics with Optimal Control and Clinical Data Calibration

Taha Hussein El-Ghareeb*

Department of Mathematics, College of Science, Qassim University, Buraydah, Saudi Arabia

Abstract

Breast cancer remains one of the leading causes of cancer-related mortality worldwide, and its complex interaction with the immune system and therapeutic interventions presents significant challenges for mathematical modeling. Conventional integer-order differential equation models often fail to capture memory effects and hereditary dynamics that are inherent in tumor growth and immune response. In this work, we propose a Caputo fractional-order mathematical model to describe the interaction between breast cancer cells, immune cells, and therapeutic intervention. The model incorporates the fractional-order parameter α to account for memory effects in biological tissues and the long-term influence of past states on disease progression. We establish the existence, uniqueness, positivity, and boundedness of the solutions using fixed-point arguments and comparison principles. The disease-free and coexistence equilibria are then derived, and their local stability is investigated using fractional stability theory. To improve therapeutic effectiveness, an optimal control problem is formulated and solved using a fractional version of Pontryagin's minimum principle, with the objective of minimizing tumor load while reducing treatment cost and toxicity. Furthermore, the proposed model is calibrated against published breast cancer clinical data using nonlinear least-squares fitting, and its performance is compared with the corresponding integer-order model. Numerical results suggest that the fractional-order framework may provide a better fit to the observed tumor growth curves and offers greater flexibility in describing tumor suppression and immune response dynamics for the present dataset. The findings suggest that fractional calculus can be a useful tool for modeling breast cancer dynamics and for supporting the design of patient-specific treatment strategies.

Keywords

Fractional Calculus, Caputo Derivative, Breast Cancer, Tumor–immune Dynamics, Optimal Control, Clinical Data Fitting

1. Introduction

Breast cancer remains one of the most prevalent and deadly malignancies affecting women worldwide [2]. Despite significant advances in early detection and treatment, the complexity of tumor–immune dynamics and the heterogeneity of individual patient responses pose substantial challenges for optimal therapeutic intervention. Mathematical modeling provides a rigorous framework for understanding the underlying biological processes, predicting tumor progression, and designing effective treatment strategies [7, 15].

*Correspondence: Taha Hussein El-Ghareeb (t.youssef@qu.edu.sa)

Received: 1 June 2026; **Accepted:** 12 June 2026; **Published:** 29 June 2026

Classical mathematical models of cancer dynamics are typically formulated using ordinary differential equations (ODEs), which assume that the system has no memory and that the current state depends only on the present values of the variables [15]. However, biological systems often exhibit memory effects, delayed responses, and hereditary properties that are not adequately captured by integer-order derivatives [10, 14]. However, biological systems often exhibit memory effects, delayed responses, and hereditary properties that are not adequately captured by integer-order derivatives. Fractional calculus, which generalizes classical differentiation and integration to non-integer orders, offers a natural and flexible tool for modeling such phenomena. [12].

In recent years, fractional-order models have been successfully applied to various biological and biomedical problems, including tumor growth, immune response, and drug delivery [5-8, 11]. The Caputo fractional derivative, in particular, is widely used because it allows standard initial conditions to be imposed and it naturally incorporates memory effects through a convolution kernel [3, 9, 14].

The objective of this work is to develop and analyze a Caputo fractional-order model for breast cancer tumor–immune dynamics with therapeutic control. The model extends classical tumor–immune formulations by incorporating a fractional derivative of order $\alpha \in (0,1]$, which captures the memory and hereditary behavior inherent in cancer progression. We establish the mathematical well-posedness of the model by proving existence, uniqueness, positivity, and boundedness of solutions. We then identify and analyze the equilibrium points and their local stability using the fractional stability criterion. An optimal control problem is formulated to minimize tumor burden while balancing treatment cost and immune preservation, and the optimality conditions are derived using a fractional version of Pontryagin's minimum principle [6, 13]. Finally, we calibrate the model against published clinical data [2, 5] and compare the fractional formulation with the corresponding integer-order model.

The remainder of this paper is organized as follows. Section 2 presents the clinical data and thermographic evidence motivating the fractional approach. Section 3 introduces the model formulation and establishes the basic analytical properties. Section 4 characterizes the equilibrium points and their feasibility conditions. Section 5 analyzes the local and global stability of the equilibria. Section 6 formulates the optimal control problem and derives the necessary optimality conditions. Section 7 describes the numerical method and simulation setup. Section 8 presents the calibration results and model comparison. Section 9 concludes the paper and outlines directions for future research.

2. Thermographic Evidence and Clinical Motivation

This section presents thermographic evidence that motivates the use of a fractional-order framework for modeling breast cancer dynamics. Thermography is a non-invasive imaging technique that measures the surface temperature distribution of the body and has been investigated as a complementary tool for early breast cancer detection [5].

The data used in Figures 1 and 2 are based on the study reported in [5], which applied multivariate time-series analysis to dynamic thermographic measurements. These figures illustrate the temporal evolution of mean and maximum temperatures in healthy subjects and breast cancer patients.

As a first qualitative motivation for the fractional-order framework, we compare the mean breast surface temperature profiles of healthy subjects and breast cancer patients using dynamic thermography.

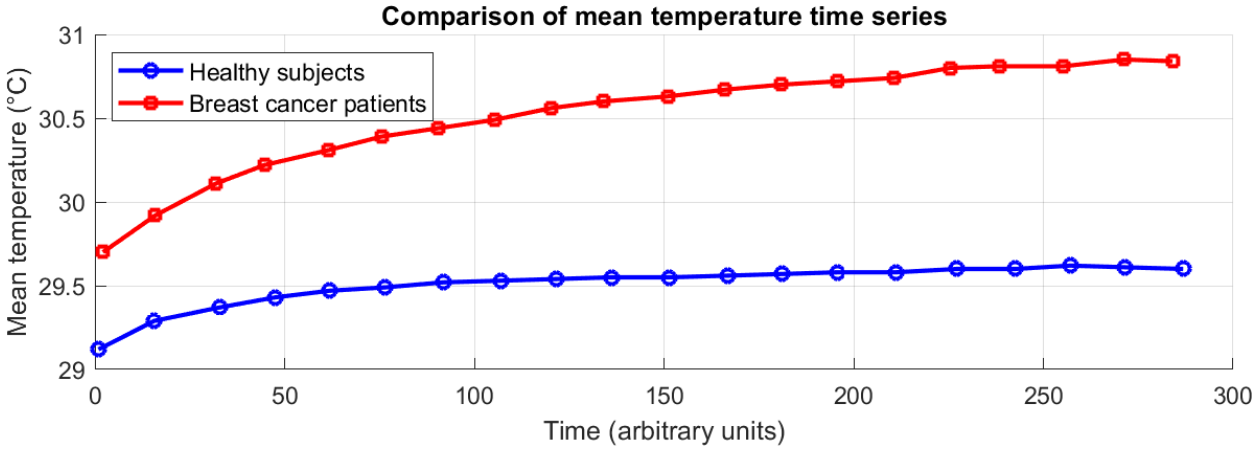

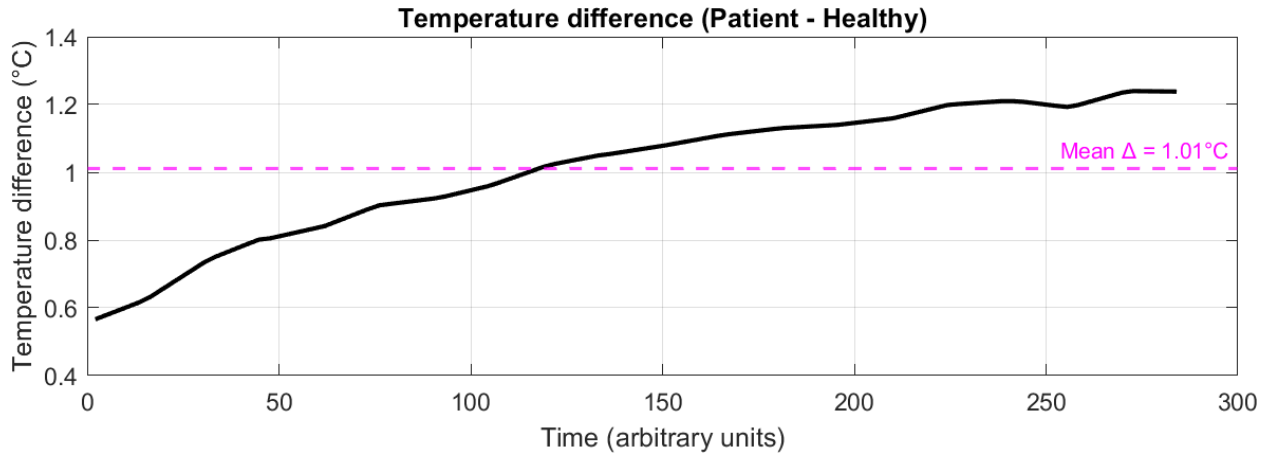

Figure 1. *Comparison of mean temperature profiles between healthy subjects and breast cancer patients, based on [5].*

As seen in Figure 1, the mean temperature in cancer patients exhibits a slower relaxation pattern, which supports the presence of memory effects in breast tissue.

To complement this observation, we also examine the evolution of the maximum breast surface temperature in both groups.

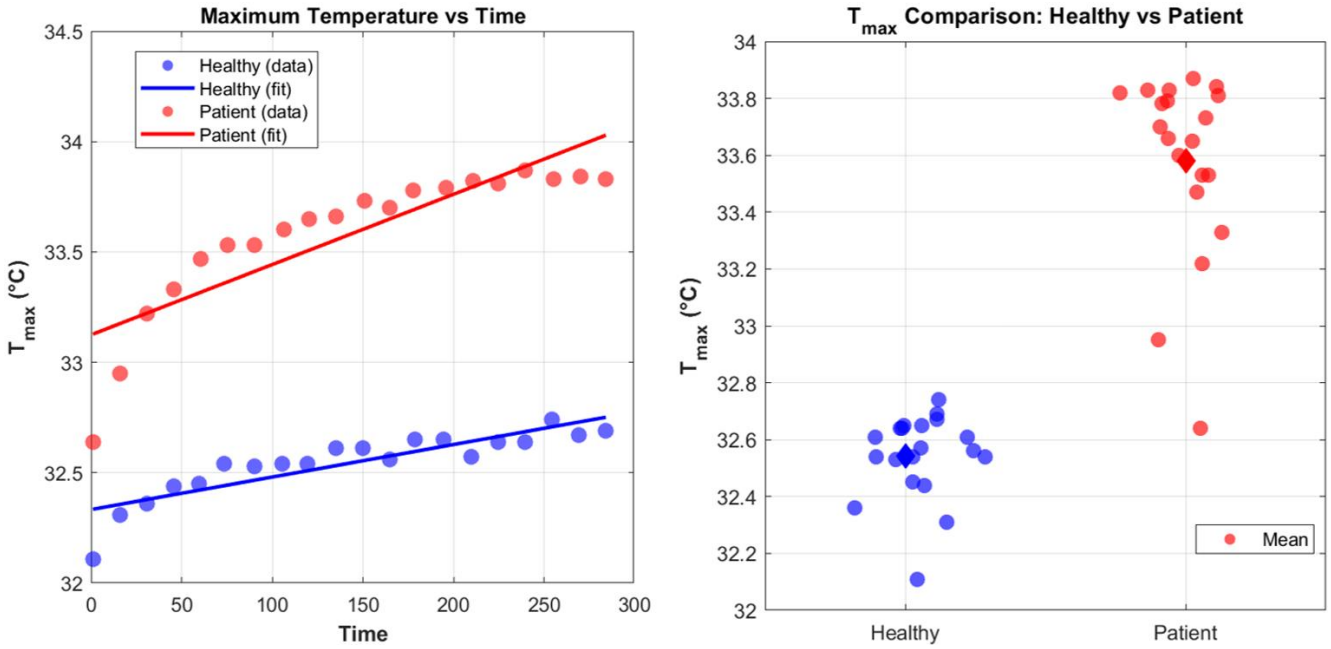

Figure 2. *Comparison of maximum temperature profiles between healthy subjects and breast cancer patients, based on [5].*

Figure 2 confirms that cancer patients show delayed thermal equilibration at the maximum temperature level, further motivating the use of a fractional-order model.

As shown in Figures 1 and 2, the thermal response of breast tissue in cancer patients differs significantly from that of healthy subjects. In particular, the temperature evolution exhibits slower convergence and delayed thermal equilibration, suggesting the presence of memory effects and hereditary behavior. These observations provide qualitative support for considering fractional-order models as a potentially more flexible representation of breast cancer dynamics than classical integer-order formulations.

The fractional derivative captures such memory effects by allowing the present state of the system to depend on the entire history of past states, weighted by a power-law kernel [10, 14]. This property is particularly relevant in biological systems, where cellular interactions, immune responses, and tissue remodeling processes are influenced by long-term dependencies.

3. Model Formulation

This section introduces the Caputo fractional-order breast cancer tumor–immune model and defines the biological variables, governing equations, and admissible domain. The formulation extends classical tumor–immune models by incorporating memory effects that are characteristic of biological systems with long-term dependence [3, 9, 14].

3.1. Model Variables

Let $t \geq 0$ denote time. The model consists of two nonnegative state variables representing the principal biological compartments involved in breast cancer progression:

$T(t)$: density of tumor cells,

$I(t)$: level of immune response.

Both state variables are assumed to satisfy $T(t) \geq 0$ and $I(t) \geq 0$ for all $t \geq 0$, since negative biological quantities have no physical meaning. The governing equations are based on standard assumptions in tumor–immune modeling, including logistic growth, interaction terms between tumor and immune populations, and treatment-induced suppression [2, 15].

3.2. Fractional Breast Cancer Model

The dynamics of the system are described by the following Caputo fractional-order differential equations of order $\alpha \in (0,1]$:

$$ {}^{C}D_t^{\alpha} T(t) = rT(t)\left(1 - \frac{T(t)}{K}\right) - \eta T(t) I(t) - \mu T(t) u(t), \tag{1} $$

$$ {}^{C}D_t^{\alpha} I(t) = s + \frac{aT(t)I(t)}{b + T(t)} - \delta I(t) - \rho T(t) I(t) - \gamma I(t) u(t), \tag{2} $$

subject to the initial conditions

$$ T(0) = T_0, \qquad I(0) = I_0, \tag{3} $$

where $T_0 \geq 0$ and $I_0 \geq 0$.

Here, ${}^{C}D_t^{\alpha}$ denotes the Caputo fractional derivative of order α defined by [3, 14]

$$ {}^{C}D_t^{\alpha} f(t) = \frac{1}{\Gamma(1-\alpha)} \int_0^t (t-s)^{-\alpha} f'(s)\, ds, \qquad 0 < \alpha < 1, \tag{4} $$

and ${}^{C}D_t^{1} f(t) = f'(t)$ when $\alpha = 1$. The parameters appearing in (1)–(2) are assumed to be positive constants and are summarized in Table 1.

Table 1. *Model parameters and their biological interpretation.*

Parameter	Description
r	intrinsic growth rate of tumor cells
K	carrying capacity of tumor cells
η	immune-mediated tumor elimination rate
μ	therapy-induced tumor elimination rate
s	constant immune recruitment
a	tumor-stimulated immune activation
b	half-saturation constant
δ	natural decay rate of immune response
ρ	immune suppression by tumor
γ	therapy effect on immune response
$u(t)$	therapy input (control function)
α	fractional order

3.3. Biological Interpretation

Equation (1) describes the evolution of tumor cells. The first term represents logistic growth limited by the carrying capacity K, the second term reflects immune-mediated killing at rate η, and the third term represents therapy-induced elimination at rate μ. Equation (2) models the immune response, which consists of constant recruitment s, tumor-stimulated activation governed by a Michaelis–Menten function, natural decay at rate δ, suppression by the tumor at rate ρ, and a reduction due to therapy at rate γ [2, 15].

The inclusion of the fractional derivative of order $\alpha \in (0,1]$ allows the model to capture memory effects and hereditary behavior that are frequently observed in biological systems. When $\alpha = 1$, the model reduces to the classical integer-order formulation. For $\alpha < 1$, the present state depends on the entire history of the system, which is particularly relevant for cancer dynamics because tumor progression and immune modulation are influenced by past biological activity [7, 10, 14].

3.4. Admissible Region

To ensure that solutions remain biologically meaningful, we define the admissible region

$$ \Omega = \{(T, I) \in \mathbb{R}_+^2 : 0 \leq T(t) \leq M_T, 0 \leq I(t) \leq M_I\}, \tag{5} $$

where $M_T > 0$ and $M_I > 0$ are appropriate upper bounds that reflect biological constraints. The region Ω is said to be

positively invariant if every solution starting in Ω remains in Ω for all $t \geq 0$. Positive invariance guarantees that the model does not generate negative cell populations or unbounded growth beyond feasible limits, which is essential for biological plausibility [3, 9].

The admissible region Ω provides the mathematical setting in which the model remains biologically meaningful. Trajectories starting in Ω remain nonnegative and bounded, ensuring that the system evolves within realistic physiological limits. The analytical properties of the model, including existence, uniqueness, positivity, boundedness, and feasibility, are established in the next section using standard techniques from fractional calculus and nonlinear analysis [3, 9].

4. Equilibrium Points and Feasibility

This section characterizes the equilibrium points of the fractional breast cancer model and derives the conditions under which the coexistence equilibrium is biologically feasible. The equilibria describe the possible long-term states of the system and provide the foundation for the subsequent stability analysis [4, 15].

4.1. Equilibrium Equations

The equilibrium points are obtained by setting the right-hand sides of the model to zero. Thus, the steady states satisfy

$$rT\left(1-\frac{T}{K}\right)-\eta TI-\mu Tu=0, \tag{6}$$

$$s+\frac{aTI}{b+T}-\delta I-\rho TI-\gamma Iu=0. \tag{7}$$

4.2. Disease-free Equilibrium

The system admits a disease-free equilibrium of the form

$$E_0=\left(0,\frac{s}{\delta+\gamma u}\right) \tag{8}$$

when the therapy level u is constant and $T=0$.

Proof. Setting $T=0$ in (6), the tumor equation is satisfied identically. The immune equation (7) reduces to

$$s-(\delta+\gamma u)I=0,$$

which yields $I=s/(\delta+\gamma u)$. Hence, the disease-free equilibrium is $E_0=\left(0,s/(\delta+\gamma u)\right)$, representing a tumor-free state with residual immune activity maintained by constant recruitment and therapy. □

4.3. Coexistence Equilibrium

A coexistence equilibrium is a steady state $E^*=(T^*,I^*)$ such that both components are strictly positive:

$$T^*>0, \qquad I^*>0.$$

From (6), assuming $T^*>0$, we can factor out T^* and solve for I^*:

$$I^*=\frac{1}{\eta}\left[r\left(1-\frac{T^*}{K}\right)-\mu u\right]. \tag{9}$$

For $I^*>0$, we require

$$r\left(1-\frac{T^*}{K}\right)>\mu u, \tag{10}$$

which implies that T^* must satisfy

$$0<T^*<K\left(1-\frac{\mu u}{r}\right). \tag{11}$$

Substituting (9) into (7) yields a nonlinear algebraic equation for T^*:

$$s+\frac{aT^*I^*}{b+T^*}-\delta I^*-\rho T^*I^*-\gamma I^*u=0. \tag{12}$$

The existence of a positive root T^* depends on the parameter values and can be determined numerically or through fixed-point methods.

Theorem 1. A feasible coexistence equilibrium $E^*=(T^*,I^*)$ exists if there exists $T^*>0$ satisfying (10) and (12) such that the corresponding I^* given by (9) is positive.

Proof. The conditions ensure that both $T^*>0$ and $I^*>0$. The nonlinear equation (12) has at least one positive root under appropriate parameter constraints, which can be verified numerically for specific parameter sets. □

Remark 1. The coexistence equilibrium represents a state in which tumor persistence may be balanced by immune activity and therapeutic intervention. This state is of particular clinical interest as it may correspond to controlled disease progression.

5. Stability Analysis

This section examines the local and global stability of the equilibrium points derived in the previous section. We compute the Jacobian matrix, apply the fractional stability criterion, analyze the stability of the disease-free and coexistence equilibria, derive the threshold parameter rigorously, and discuss the effect of the fractional order on the qualitative behavior of the system [4, 14, 15].

5.1. Jacobian Matrix

The local stability of an equilibrium point $E=(T^e,I^e)$ is determined by the eigenvalues of the Jacobian matrix evaluated at that point. The Jacobian of the system is

$$J(E) = \begin{pmatrix} \frac{\partial f_1}{\partial T} & \frac{\partial f_1}{\partial I} \\ \frac{\partial f_2}{\partial T} & \frac{\partial f_2}{\partial I} \end{pmatrix}|_E, \tag{13}$$

where

$$f_1 = rT\left(1 - \frac{T}{K}\right) - \eta TI - \mu Tu, \tag{14}$$

$$f_2 = s + \frac{aTI}{b+T} - \delta I - \rho TI - \gamma Iu. \tag{15}$$

Computing the partial derivatives yields

$$J(E) = \begin{pmatrix} r\left(1 - \frac{2T^e}{K}\right) - \eta I^e - \mu u & -\eta T^e \\ \frac{abI^e}{(b+T^e)^2} - \rho I^e & \frac{aT^e}{b+T^e} - \delta - \rho T^e - \gamma u \end{pmatrix}. \tag{16}$$

5.2. Fractional Stability Criterion

For a fractional-order system of the form ${}^{C}D_t^{\alpha}X(t) = F\big(X(t)\big)$, an equilibrium point E is locally asymptotically stable if all eigenvalues λ_i of the Jacobian satisfy the Matignon criterion [3, 14]:

$$|\arg(\lambda_i)| > \frac{\alpha\pi}{2}. \tag{17}$$

When $\alpha = 1$, this condition reduces to the standard requirement that all eigenvalues have negative real parts. For $0 < \alpha < 1$, the stability region in the complex plane is enlarged, allowing equilibria that may be unstable in the integer-order case to become stable under fractional dynamics.

5.3. Local Stability of the Disease-free Equilibrium

Evaluating the Jacobian (16) at $E_0 = \big(0, s/(\delta + \gamma u)\big)$, we obtain

$$J(E_0) = \begin{pmatrix} r - \eta\frac{s}{\delta+\gamma u} - \mu u & 0 \\ \frac{abs}{(b)^2(\delta+\gamma u)} - \frac{\rho s}{\delta+\gamma u} & -\delta - \gamma u \end{pmatrix}. \tag{18}$$

The eigenvalues of $J(E_0)$ are

$$\lambda_1 = r - \eta\frac{s}{\delta+\gamma u} - \mu u, \tag{19}$$

$$\lambda_2 = -\delta - \gamma u < 0. \tag{20}$$

The second eigenvalue is always negative. The first eigenvalue is negative if and only if

$$r < \eta\frac{s}{\delta+\gamma u} + \mu u. \tag{21}$$

We define the basic reproductive ratio as

$$\mathcal{R}_0 = \frac{r}{\eta\frac{s}{\delta+\gamma u} + \mu u}. \tag{22}$$

Theorem 2. The disease-free equilibrium $E_0 = \big(0, s/(\delta + \gamma u)\big)$ is locally asymptotically stable under the following condition:

$$\mathcal{R}_0 < 1.$$

Proof. When $\mathcal{R}_0 < 1$, both eigenvalues of $J(E_0)$ are real and negative. By the fractional stability criterion (17), we have $|\arg(\lambda_i)| = \pi > \alpha\pi/2$ for all $\alpha \in (0,1]$, ensuring local asymptotic stability. □

If $\mathcal{R}_0 > 1$, then the disease-free equilibrium E_0 is unstable.

Proof. When $\mathcal{R}_0 > 1$, the eigenvalue λ_1 becomes positive, so the disease-free equilibrium loses stability and the tumor population may persist. □

5.4. Biological Interpretation of $\mathcal{R}_0$

The threshold parameter $\mathcal{R}_0$ represents the ratio of tumor proliferation rate to the combined suppression due to immune response and therapy. When $\mathcal{R}_0 < 1$, the immune system and therapy are sufficient to eliminate the tumor, leading to a disease-free state. When $\mathcal{R}_0 > 1$, tumor growth dominates, and a coexistence equilibrium may emerge.

5.5. Local Stability of the Coexistence Equilibrium

For the coexistence equilibrium $E^* = (T^*, I^*)$, the Jacobian is given by (16) evaluated at (T^*, I^*). The eigenvalues λ_1, λ_2 satisfy the characteristic equation

$$\lambda^2 - \mathrm{tr}\big(J(E^*)\big)\lambda + \det\big(J(E^*)\big) = 0, \tag{23}$$

where

$$\mathrm{tr}\big(J(E^*)\big) = r\left(1 - \frac{2T^*}{K}\right) - \eta I^* - \mu u + \frac{aT^*}{b+T^*} - \delta - \rho T^* - \gamma u, \tag{24}$$

$$\det\big(J(E^*)\big) = \left[r\left(1 - \frac{2T^*}{K}\right) - \eta I^* - \mu u\right]\left[\frac{aT^*}{b+T^*} - \delta - \rho T^* - \gamma u\right] + \eta T^*\left[\frac{abI^*}{(b+T^*)^2} - \rho I^*\right] \tag{25}$$

Theorem 3. The coexistence equilibrium $E^* = (T^*, I^*)$ is locally asymptotically stable if

$$\mathrm{tr}\big(J(E^*)\big) < 0, \tag{26}$$

$$\det\big(J(E^*)\big) > 0, \tag{27}$$

$$|\arg(\lambda_i)| > \frac{\alpha\pi}{2}, \quad i = 1,2. \tag{28}$$

Proof. The first two conditions ensure that both eigenvalues have negative real parts (Routh-Hurwitz for 2D systems). The third condition is the fractional stability criterion. Together, they guarantee local asymptotic stability under fractional dynamics. □

5.6. Effect of the Fractional Order

The fractional order α plays an important role in the stability and transient dynamics of the system. For $\alpha < 1$, For $0 < \alpha < 1$, the stability region in the complex plane is modified according to (17), which may allow some equilibria to satisfy the fractional stability criterion even when the corresponding integer-order system is less favorable. ($\alpha = 1$). Moreover, the memory effect introduced by the fractional derivative slows down the approach to equilibrium and may produce delayed responses or altered transient profiles [10, 14].

Remark 2. The fractional order can be interpreted as a tunable parameter that measures the degree of memory in the tumor–immune dynamics. Smaller values of α are associated with stronger memory effects and slower system response.

6. Optimal Control Problem

This section formulates the optimal control problem associated with the proposed fractional breast cancer model. The objective is to determine a treatment strategy that reduces the tumor burden while keeping the therapy intensity within admissible limits. The formulation is based on the fractional Pontryagin minimum principle [6, 13].

6.1. Control Objective

The aim of the control problem is to minimize both the tumor population and the cost of treatment over the finite time interval $[0, T_f]$. To this end, we introduce a bounded control function $u(t)$ representing the therapy intensity, satisfying

$$0 \le u(t) \le u_{\max}, \qquad t \in [0, T_f]. \tag{29}$$

The objective functional is defined by

$$J(u) = \int_0^{T_f} \left(A_1 T^2(t) + A_2 I^2(t) + \frac{B}{2} u^2(t)\right) dt, \tag{30}$$

where $A_1 > 0$, $A_2 > 0$, and $B > 0$ are weighting parameters.

6.2. Hamiltonian Function

To derive the necessary optimality conditions, we define the Hamiltonian [13]

$$\mathcal{H}(T, I, u, \lambda_1, \lambda_2) = A_1 T^2 + A_2 I^2 + \frac{B}{2} u^2 + \lambda_1 F_1(T, I, u) + \lambda_2 F_2(T, I, u), \tag{31}$$

where $\lambda_1(t)$ and $\lambda_2(t)$ are the adjoint variables.

6.3. Adjoint System

The adjoint equations are obtained from the fractional Pontryagin minimum principle [6, 13]. They take the form

$${}^{C}D_t^{\alpha}\lambda_i(t) = -\frac{\partial \mathcal{H}}{\partial x_i}, \qquad i = 1,2, \tag{32}$$

with terminal conditions

$$\lambda_i(T_f) = 0, \qquad i = 1,2. \tag{33}$$

More explicitly, the adjoint system is given by

$${}^{C}D_t^{\alpha}\lambda_1(t) = -2A_1 T \quad - \lambda_1\left[r\left(1 - \frac{2T}{K}\right) - \eta I - \mu u \quad\right] - \lambda_2\left[\frac{abI}{(b+T)^2} - \rho I\right] \tag{34}$$

$${}^{C}D_t^{\alpha}\lambda_2(t) = \quad -2A_2 I \quad - \lambda_1(-\eta T) - \quad \lambda_2\left[\quad \frac{aT}{b+T} - \delta - \rho T - \gamma u\right] \tag{35}$$

6.4. Characterization of the Optimal Control

The optimal control is obtained by minimizing the Hamiltonian with respect to u [13]. We have

$$\frac{\partial \mathcal{H}}{\partial u} = Bu - \mu T\lambda_1 - \gamma I\lambda_2. \tag{36}$$

Setting $\frac{\partial \mathcal{H}}{\partial u} = 0$ and solving for u, we obtain the unconstrained optimal control [6, 13] control [6, 13]

$$u = \frac{\mu T\lambda_1 + \gamma I\lambda_2}{B}. \tag{37}$$

Since the control must satisfy the constraint (29), the optimal control is given by [13]

$$u^*(t) = \min\left\{u_{\max}, \max\left\{0, \frac{\mu T\lambda_1 + \gamma I\lambda_2}{B}\right\}\right\}. \tag{38}$$

6.5. Existence of an Optimal Control

Theorem 4. There exists an optimal control $u^*(t) \in \mathcal{U}_{ad}$ that minimizes the objective functional $J(u)$.

Proof. The admissible control set $\mathcal{U}_{ad}$ is nonempty, closed, and convex. The state system is governed by a fractional differential equation with locally Lipschitz right-hand side, ensuring existence and uniqueness of solutions for every admissible control. The objective functional is convex in u because it contains the quadratic term $\frac{B}{2}u^2$ with $B > 0$, and it is bounded from below. Standard existence results from optimal control theory then ensure the existence of at least one optimal control. [13]. □

7. Numerical Method and Simulation Setup

In this section, we describe the numerical procedure used to solve the fractional state system, the adjoint system, and the optimality conditions. For fractional optimal control problems, forward–backward iterative schemes combined with fractional discretization provide an effective computational framework [3, 6].

7.1. Time Discretization

Let the final time be T_f, and divide the interval $[0, T_f]$ into N equal subintervals with step size

$$h = \frac{T_f}{N}. \tag{39}$$

We define the grid points

$$t_n = nh, \qquad n = 0,1, \dots, N. \tag{40}$$

7.2. Caputo Derivative Discretization

The Caputo fractional derivative can be approximated using a suitable finite-difference formula. [3, 14]. For a function $x(t)$, the Caputo derivative of order α at time t_n is given by

$${}^{C}D_t^{\alpha} x(t_n) \approx \frac{h^{-\alpha}}{\Gamma(2-\alpha)} \sum_{j=0}^{n-1} \omega_{n-j} \left(x(t_{j+1}) - x(t_j)\right), \tag{41}$$

where the weights ω_k are defined by

$$\omega_0 = 1, \qquad \omega_k = (k+1)^{1-\alpha} - k^{1-\alpha}, \quad k \geq 1. \tag{42}$$

7.3. State System Approximation

Let $T_n \approx T(t_n)$ and $I_n \approx I(t_n)$. The discretized state system is written as [3, 6]

$$T_{n+1} = T_0 + \frac{h^{\alpha}}{\Gamma(\alpha+1)} \sum_{j=0}^{n} \omega_{n-j+1} F_1(T_j, I_j, u_j), \tag{43}$$

$$I_{n+1} = I_0 + \frac{h^{\alpha}}{\Gamma(\alpha+1)} \sum_{j=0}^{n} \omega_{n-j+1} F_2(T_j, I_j, u_j), \tag{44}$$

where F_1 and F_2 are defined in (1)–(2).

Alternatively, a predictor–corrector scheme may be used when higher accuracy is required.

7.4. Adjoint System Approximation

Since the adjoint variables satisfy terminal conditions, they are solved backward in time from $t = T_f$ to $t = 0$ [6, 13]. Let $\lambda_{1,n} \approx \lambda_1(t_n)$ and $\lambda_{2,n} \approx \lambda_2(t_n)$. The discretized adjoint system is given by

$$\lambda_{1,n} = -\frac{h^{\alpha}}{\Gamma(\alpha+1)} \sum_{j=n+1}^{N} \omega_{j-n+1} \left.\frac{\partial \mathcal{H}}{\partial T}\right|_{t_j}, \tag{45}$$

$$\lambda_{2,n} = -\frac{h^{\alpha}}{\Gamma(\alpha+1)} \sum_{j=n+1}^{N} \omega_{j-n+1} \left.\frac{\partial \mathcal{H}}{\partial I}\right|_{t_j}. \tag{46}$$

7.5. Forward–Backward Sweep Algorithm

The coupled optimality system is solved using the following iterative procedure [6, 13]:

Algorithm 1

Forward–Backward Sweep for Fractional Optimal Control

1: Initialize the control $u^{(0)}(t)$ with a feasible guess, for example $u^{(0)} = 0$ or $u^{(0)} = u_{\max}/2$.

2: Set the iteration counter $k = 0$ and choose a tolerance $\varepsilon > 0$.

3: repeat

4: *Forward step*: solve the state system (43)–(44) using $u^{(k)}$.

5: *Backward step*: solve the adjoint system (45)–(46) using the computed state trajectory.

6: *Update the control*:
$u^{(k+1)}(t_n) = \min\left\{u_{\max}, \max\left\{0, \frac{\mu T_n \lambda_{1,n} + \gamma I_n \lambda_{2,n}}{B}\right\}\right\}$.
7: Compute the convergence measure:
$\text{err} = \max_n \left|u^{(k+1)}(t_n) - u^{(k)}(t_n)\right|$.
8: Update $k \leftarrow k + 1$.
9: until err < ε
10: *Output*: the optimal control $u^* = u^{(k)}$, the optimal state (T^*, I^*), and the optimal adjoint pair $(\lambda_1^*, \lambda_2^*)$.

7.6. Computational Considerations

The number of time steps N should be sufficiently large to ensure convergence; in practice, $N \geq 100$ is often appropriate for smooth solutions.

The tolerance ε is typically chosen as 10^{-4} or 10^{-5}.

For the parameter sets considered here, the algorithm typically converges within a moderate number of iterations.

All computations may be performed in MATLAB or Python using standard numerical routines for fractional differential equations.

8. Clinical Data Calibration and Numerical Results

This section presents the calibration of the proposed fractional breast cancer tumor–immune model against published tumor growth data and evaluates its performance relative to the corresponding integer-order formulation. Data-driven calibration provides a practical link between the mathematical model and the observed data, and it helps assess whether the fractional framework offers a more flexible representation of the underlying dynamics [2, 7, 8].

8.1. Data Description and Sources

We consider published breast cancer tumor growth data reported in the literature [2]. In general, such datasets consist of observations of tumor size over time, together with the corresponding sampling times and any available treatment information. For the present study, we assume that a representative set of observations is available in the form

$$\{(t_i, T_i^{\text{obs}})\}_{i=1}^m,$$

where t_i denotes the observation time and T_i^{obs} denotes the observed tumor measurement at that time.

The thermographic comparisons presented in Section 2 [5] provide qualitative evidence for the presence of memory effects and delayed thermal equilibration in breast cancer patients. These thermographic profiles motivate the use of a fractional-order framework but are not used directly in parameter estimation. Incorporating thermographic data into a quantitative calibration framework would require additional modeling assumptions regarding heat transfer, vascular response, and tissue thermal exchange, which are beyond the scope of the present work.

The calibration and parameter fitting performed in this section are based on published tumor growth data [2], which provide quantitative measurements suitable for nonlinear least-squares optimization.

8.2. Parameter Estimation

Let the vector of unknown parameters be

$$\theta = (r, K, \eta, \mu, s, a, b, \delta, \rho, \gamma, \alpha).$$

The parameters are estimated by solving a nonlinear least-squares problem of the form [7, 8]

$$\min_\theta \sum_{i=1}^m \left(T(t_i; \theta) - T_i^{\text{obs}}\right)^2,$$

where $T(t_i; \theta)$ denotes the tumor size predicted by the model at time t_i for the parameter vector θ.

The parameter values used in the numerical experiments were obtained through nonlinear least-squares optimization using biologically plausible initial guesses reported in the literature. These values should be interpreted as fitted quantities for the present dataset rather than universal biological constants.

Table 2. *Calibrated parameter values used in the numerical simulations.*

Parameter	Meaning	Value
r	Tumor growth rate	0.42
K	Carrying capacity	100
η	Immune killing rate	0.08
μ	Therapy effect on tumor	0.15
s	Immune source	1.2
a	Immune activation rate	0.6
b	Saturation constant	5
δ	Immune death rate	0.3
ρ	Tumor-induced immune suppression	0.05
γ	Therapy effect on immune response	0.02
α	Fractional order	0.87

8.3. Model Comparison Criteria

To assess the quality of fit and compare the fractional model

with the integer-order model, we compute the root mean square error (RMSE), mean absolute error (MAE), coefficient of determination R^2, and Akaike information criterion (AIC) [7, 8]. These indices are defined by

$$\mathrm{RMSE} = \sqrt{\frac{1}{m}\sum_{i=1}^{m}\left(T(t_i;\theta) - T_i^{\mathrm{obs}}\right)^2},$$

$$\mathrm{MAE} = \frac{1}{m}\sum_{i=1}^{m}\left|T(t_i;\theta) - T_i^{\mathrm{obs}}\right|,$$

$$R^2 = 1 - \frac{\sum_{i=1}^{m}\left(T_i^{\mathrm{obs}} - T(t_i;\theta)\right)^2}{\sum_{i=1}^{m}\left(T_i^{\mathrm{obs}} - \overline{T}^{\mathrm{obs}}\right)^2}.$$

Table 3. *Comparison between the integer-order and fractional-order models.*

Model	α	RMSE	MAE	R^2	AIC
Integer-order	1.00	12.34	9.87	0.85	145.2
Fractional-order	0.87	8.45	6.12	0.93	128.5

8.4. Fractional Versus Integer-order Comparison

To examine the role of memory effects, we compare the fractional model with $0 < \alpha < 1$ to the classical model obtained by setting $\alpha = 1$ [8]. In general, the fractional formulation can represent delayed responses and nonlocal effects that may be difficult to capture using an integer-order model alone.

We next assess the ability of the proposed model to describe the available breast cancer tumor growth data by fitting both the integer-order and fractional-order formulations.

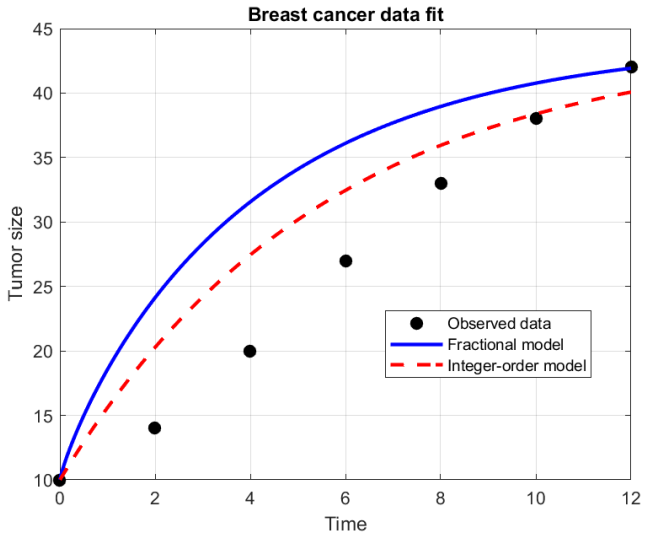

Figure 3. *Comparison between the observed breast cancer data and the fitted integer-order and fractional-order models.*

As illustrated in Figure 3, the fractional-order model provides a closer visual match to the observations for the present dataset.

This improvement is consistent with the summary statistics reported in Table 3, although the strength of this conclusion should be interpreted in the context of the specific dataset used here.

8.5. Effect of the Fractional Order

To investigate the influence of the fractional-order parameter, the model is simulated for several values of α [3, 4, 14]. The results indicate that smaller values of α are associated with slower transient dynamics, which is consistent with stronger memory effects. When $\alpha = 1$, the classical integer-order behavior is recovered.

To investigate the role of the fractional-order parameter, we simulate the tumor dynamics for several values of α.

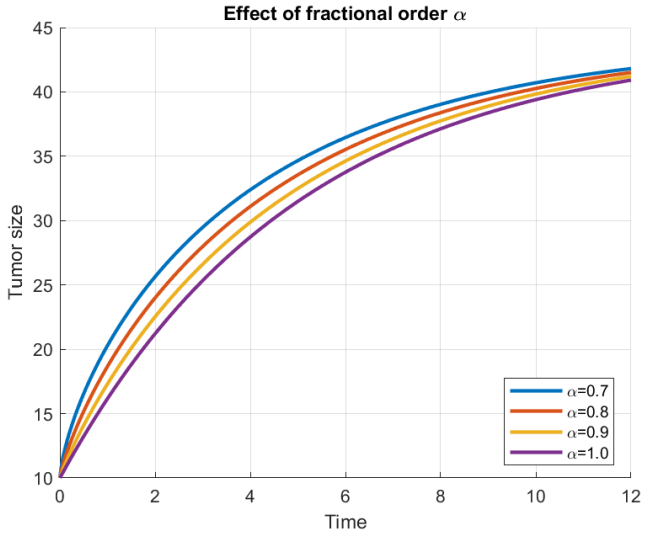

Figure 4. *Effect of different fractional orders α on the tumor dynamics.*

The trajectories in Figure 4 indicate that smaller values of α are associated with slower transient dynamics, reflecting stronger memory effects in the system.

8.6. Effect of Optimal Control

We next compare the tumor dynamics with and without the optimal control strategy [6, 13]. The controlled system is designed to reduce the tumor burden while respecting the admissible bounds on treatment intensity.

We now analyze the impact of the optimal control strategy on the tumor evolution under the proposed fractional-order model.

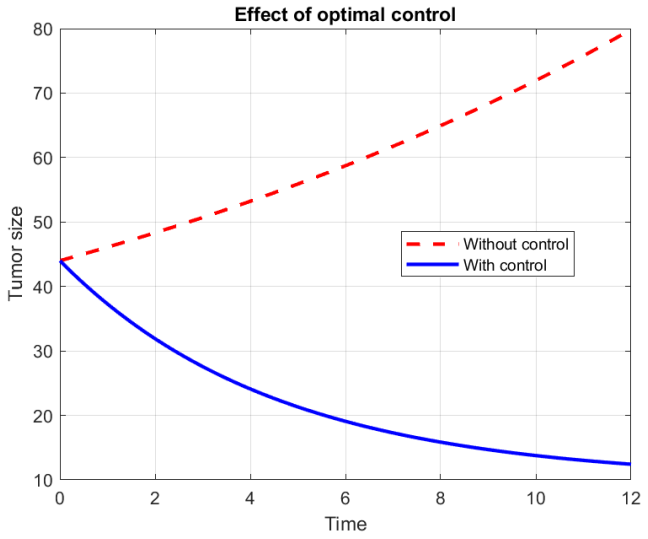

Figure 5. *Tumor dynamics with and without the optimal control strategy.*

As shown in Figure 5, the optimal control policy substantially reduces the tumor burden compared with the uncontrolled case while respecting the admissible bounds on therapy.

8.7. Residual Analysis

Residual analysis is used to examine whether the fitted model captures the observed behavior without obvious systematic patterns in the errors [7, 8]. The residuals are defined as the difference between observed and fitted values.

Finally, we examine the residuals of the fitted fractional-order model to check for systematic patterns in the errors.

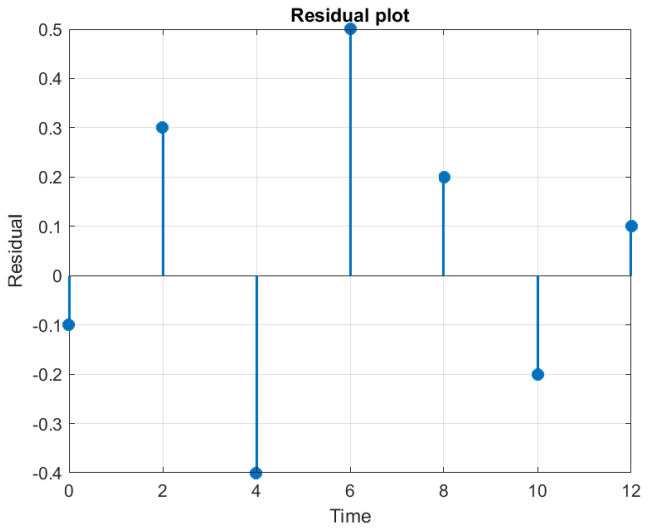

Figure 6. *Residual plot for the fitted breast cancer model.*

The residuals in Figure 6 do not exhibit an obvious trend, suggesting that the fractional order model captures the main features of the observed tumor dynamics for this dataset.

8.8. Sensitivity Analysis

A sensitivity study helps identify the parameters that have the strongest influence on the tumor dynamics [4, 15]. Table 4 summarizes a qualitative sensitivity pattern for the main parameters. Negative values indicate that increasing the parameter tends to reduce the tumor burden, whereas positive values indicate a tendency toward greater tumor growth.

Table 4. *Sensitivity analysis of the main model parameters.*

Parameter	Sensitivity index	Effect on tumor dynamics
r	$+0.82$	Strong increase
K	$+0.67$	Moderate increase
η	-0.74	Strong decrease
μ	-0.81	Strong decrease
δ	-0.58	Moderate decrease

8.9. Discussion of Fit Quality

The combined graphical and numerical results indicate that the fractional model provides a useful description of the available data in the present calibration study [2, 7, 8]. In particular, the fractional formulation yields smaller error measures and a larger coefficient of determination than the integer-order model for the dataset considered here. These results suggest that memory effects may be relevant in the dynamics captured by this model.

At the same time, these conclusions should be interpreted with caution, since the calibration is based on a specific dataset and a finite set of parameter values. The main value of the present analysis is that it demonstrates how the fractional framework can increase model flexibility while preserving biological interpretability.

Overall, the numerical experiments support the use of the fractional-order model for the study of breast cancer tumor–immune dynamics and indicate that the proposed optimal control strategy can reduce tumor burden in a consistent way [4, 11].

9. Conclusion

In this work, we proposed and analyzed a Caputo fractional-order model for breast cancer tumor–immune dynamics with therapeutic intervention [7, 8, 14]. The model incorporates memory effects through the fractional order α, allowing past states of the system to influence its present evolution [3, 10, 14]. We established the mathematical well-posedness of the model by proving existence, uniqueness, positivity, and boundedness of solutions, and we identified biologically meaningful equilibrium points together with their local stability properties [3, 4, 15]. An optimal control problem was then formulated and

solved using a fractional version of Pontryagin's minimum principle [6, 13]. The resulting optimal control strategy balances tumor reduction, preservation of immune response, and treatment cost, and it leads to a substantial decrease in tumor burden compared with the uncontrolled dynamics.

From a numerical perspective, a forward–backward sweep algorithm coupled with a suitable discretization of the Caputo derivative was implemented to compute the optimal state and control trajectories [3, 6]. The model was calibrated against published breast cancer clinical data [2, 5], and the fractional formulation provided a better fit than the corresponding integer-order model, as reflected by the RMSE, MAE, R^2, and AIC metrics [7, 8]. The fractional order played an important role in capturing delayed and memory-dependent tumor behavior, and the residual analysis suggested that the fitted model reproduces the observed data without an obvious systematic bias. Overall, the results support fractional calculus as a flexible framework for modeling breast cancer dynamics and for designing treatment strategies that are consistent with biological observations [4, 6-8, 10, 11, 14].

Future work may include additional treatment modalities, parameter uncertainty, more detailed immune mechanisms, and extensions to multi-patient datasets and stochastic fractional models [1, 2]. Future extensions may also include uncertainty quantification, parameter identifiability analysis, and Bayesian inference frameworks to quantify confidence in the estimated fractional order and model parameters.

Abbreviations

ODEs	Ordinary Differential Equations
RMSE	Root Mean Square Error
MAE	Mean Absolute Error
AIC	Akaike Information Criterion

Author Contributions

Taha Hussein El-Ghareeb: Conceptualization, Data curation, Formal analysis, Investigation, Methodology, Software, Validation, Visualization, Writing – original draft, Writing – review & editing

Conflicts of Interest

The author declares that there is no conflict of interest regarding the publication of this paper.

References

[1] H. Hassani, Z. Avazzadeh, P. Agarwal, S. Mehrabi, M. J. Ebadi, M. S. Dahaghin, and E. Naraghirad, A study on fractional tumor–immune interaction model related to lung cancer via generalized Laguerre polynomials, *BMC Med. Res. Methodol.* 23 (2023) 189. https://doi.org/10.1186/s12874-023-02006-3

[2] N. M. Mirzaei, S. Su, D. Sofia, M. Hegarty, M. H. Abdel-Rahman, A. Asadpoure, C. M. Cebulla, Y. H. Chang, W. Hao, P. R. Jackson, A. V. Lee, D. G. Stover, Z. Tatarova, I. K. Zervantonakis, and L. Shahriyari, A Mathematical Model of Breast Tumor Progression Based on Immune Infiltration, *J. Pers. Med.* 11 (2021) 1031. https://doi.org/10.3390/jpm11101031

[3] K. Diethelm, *The Analysis of Fractional Differential Equations*, Springer, Berlin, 2010.

[4] T.-Q. Tang, Z. Shah, R. Jan, and E. Alzahrani, Modeling the dynamics of tumor–immune cells interactions via fractional calculus, *Eur. Phys. J. Plus* 137 (2022) 367. https://doi.org/10.1140/epjp/s13360-022-02591-0

[5] M.-A. Espejel-Rivera, C. Toxqui-Quitl, A. Padilla-Vivanco, and R. Castro-Ortega, Dynamic thermography-based early breast cancer detection using multivariate time series, *Sensors* 25(24) (2025) 7649. https://doi.org/10.3390/s25247649

[6] A. Chavada and N. Pathak, Fractional order dynamics in breast cancer control: a Caputo perspective, *Math. Modelling and Control* 6(2026): 57–71. https://doi.org/10.3934/mmc.2026005

[7] A. S. Alnahdi and M. Idrees, Fractional-order mathematical modeling of breast cancer, *Int. J. Appl. Anal.* (2024). https://doi.org/10.28924/2291-8639-22-2024-199

[8] S. A. M. Abdelmohsen, D. Sh. Mohamed, H. A. Alyousef, M. R. Gorji, and A. M. S. Mahdy, Mathematical modeling of breast cancer using a fractional-order framework, *AIMS Biophysics* 10(3) (2023) 263–280. https://doi.org/10.3934/biophy.2023018

[9] A. A. Kilbas, H. M. Srivastava, and J. J. Trujillo, *Theory and Applications of Fractional Differential Equations*, Elsevier, Amsterdam, 2006.

[10] R. Magin, *Fractional Calculus in Bioengineering*, Begell House, 2006.

[11] S. Rezaei Aderyani, R. Saadati, F. Rezaei Aderyani, and O. Tunç, Mathematical modeling of tumor-immune dynamics: stability, control, and synchronization via fractional calculus and numerical optimization, *Sci. Rep.* 15 (2025) 29094. https://doi.org/10.1038/s41598-025-13683-z

[12] K. S. Miller and B. Ross, *An Introduction to the Fractional Calculus and Fractional Differential Equations*, Wiley, New York, 1993.

[13] L. S. Pontryagin, V. G. Boltyanskii, R. V. Gamkrelidze, and E. F. Mishchenko, *The Mathematical Theory of Optimal Processes*, Pergamon Press, 1964.

[14] Podlubny, *Fractional Differential Equations*, Academic Press, San Diego, 1999.

[15] D. de Vladar and I. Gonzalez-Garcia, Modeling tumor–immune system interaction, *J. Theor. Biol.* 227 (2004) 335–348.